Investigation and Improvement of Molten Zinc Corrosion of a Sink Roll with Thermal Sprayed WC-Co Coating

TSAI-SHANG HUANG

Green Energy & System Integration Research & Development Department, China Steel Corporation

Surface treatment for sink rolls in a continuous galvanizing line is an important issue due to the hostile environment of the molten zinc. This study investigated the corrosion behavior of the WC-Co coating in molten zinc. Samples with the WC-Co coating were tested in a zinc pot and were cross-sectioned to examine the microstructure and corrosion morphology. The WC-Co coating defects on a used sink roll were also investigated and compared. The results showed that molten zinc intruded through cracks to attack the substrate which caused major destruction of the WC-Co coating. CSC has developed a special process to solve this problem and has greatly improved the service life of a sink roll.

Keywords: Molten Zinc, Corrosion, WC-Co, Sink Roll, HVOF

1. INTRODUCTION

Galvanized steel sheet is widely used in daily life due to its good corrosion resistance. In a continuous hot-dip process, pot rolls, including a sink roll and two stabilizer rolls, are operated inside the zinc pot to guide the steel sheets[1]. Zinc is then coated on both sides of the steel sheets within a few seconds. The sink roll plays the major role in directing the sheet into the pot and then changing the sheet direction to leave vertically upward. There is a large area contact by the sheet and the sink roll. A variety of groove patterns and pitches have been applied to the sink roll to decrease tendency of sheet slip. Two stabilizer rolls have slight contact with the sheet and the groove pattern is usually not necessary. These pot rolls are immersed in the molten zinc pot for a long period of time. Therefore, the roll surface degrades due to corrosion and results in the build-up of dross particles[2]. Because the steel sheet is in direct contact with the pot rolls, any defect on the roll surface will seriously affect the quality of the galvanization.

Metallic materials like Fe-based alloy and Co-based alloy, carbides like WC-Co, and oxides like Al_2O_3 and ZrO_2, have been developed as coating materials for pot rolls to resist the corrosion from the molten zinc[1,3,4,5,6,7,8,9]. WC-Co coating, usually prepared by a high velocity oxygen fuel (HVOF) spray process, is the most common solution due to its superior corrosion resistance relative to Fe and Co alloys[6]. The durability of thermal sprayed WC-Co coating in molten zinc as well as the reaction between the coating and the molten zinc has been reported [8,10,11]. Inter-diffusion of Co and Zn is suggested as the major corrosion mechanism for WC-Co coatings in molten zinc. The Presence of η phase (e.g., Co_3W_3C and Co_6W_6C) was reported to further retard the inter-diffusion rate more than the pure Co phase in the WC-Co coatings.

However, the actual failure of a sink roll usually appears as pits or coating spallation instead of thinning of the coating. In this study, samples with thermal sprayed WC-Co coating were tested in the zinc pot. Corrosion morphology was carefully examined and analyzed. The molten zinc corrosion mechanism of the WC-Co coating was proposed and the failure of a WC-Co coated sink roll is explained.

2. EXPERIMENTAL METHOD

The thermal spray powder used on the samples in this study is shown in Table 1. This powder is agglomerated and sintered. Its morphology is shown in Fig.1. Substrate of the samples is SUS 316 stainless steel with the size of 45 mm × 25 mm × 5 mm. A Sulzer Metco Diamond Jet DJ2700 HVOF gun was used to spray the WC-Co coating on the samples. Spray parameters are listed in Table 2. They were grit-blasted before thermal spraying. After thermal spraying, a silica-based sealant was applied to the coating.

Hardness and porosity of the coating were measured to ensure that they were sprayed in good conditions. Cross-sectional micro-hardness was performed by means

of Vickers indentation (Matsuzawa MXT50) at a load of 300 g for 15 sec. Porosity was quantified by using Photoshop software. Phases of the coating were analyzed by Bruker D8 Advance X-ray diffraction at a scan rate of 0.01 °/sec.

The molten zinc corrosion test was conducted in the zinc pot of a continuous galvanizing line (CGL). Samples were welded to the sides of a sink roll, as shown in Fig.2. They were immersed in the zinc pot along with the sink roll. A testing cycle is from 10 to 21 days, depending on the CGL production schedule or production condition. The aluminum content in the zinc pot is less than 2 %. After each testing cycle, samples along with the sink roll were pickled in a dilute phosphoric acid solution to remove zinc and zinc dross. The surface condition of the sink roll was examined before the next production cycle. If the surface condition was poor, the sink roll would be sent to the spray shop for repair and the samples will be removed to another sink roll for continuing testing. The total testing time of the samples was 42 days before they were sectioned and analyzed.

Cross-sections of the coating were examined under a scanning electron microscope (SEM) to reveal the corrosion morphologies. Elemental mappings of the corroded areas were performed by an electron probe micro-analyzer (EPMA).

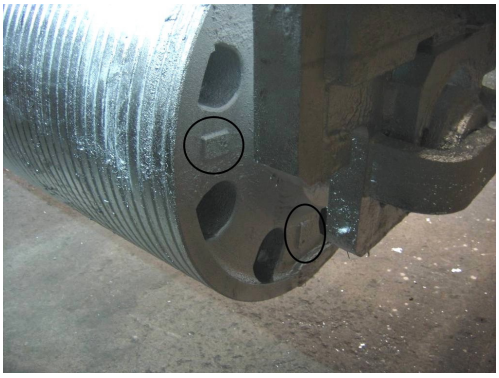

Fig.2. The circled areas show the testing samples which were welded on a sink roll.

3. RESULTS AND DISCUSSION

3.1 Coating Properties

The cross-sectional microstructure of the WC-Co coating is shown in Fig.3. The thickness of the coating is about 75*μm*. WC particles were clearly distributed in

Table 1 Details of thermal spray powders.

Powder ID	Manufacturer	Composition	Powder size
Infralloy S7412	Inframat	WC-12 wt.% Co	-45+5μm

Table 2 Spray parameters.

Oxygen (O_2)	150 psi, 38 FMR
Propylene (C_3H_6)	105 psi, 38 FMR
Air	105 psi, 48 FMR
Spray Distance	230 mm
Spray Rate	38 g/min

Note: FMR, flow meter reading

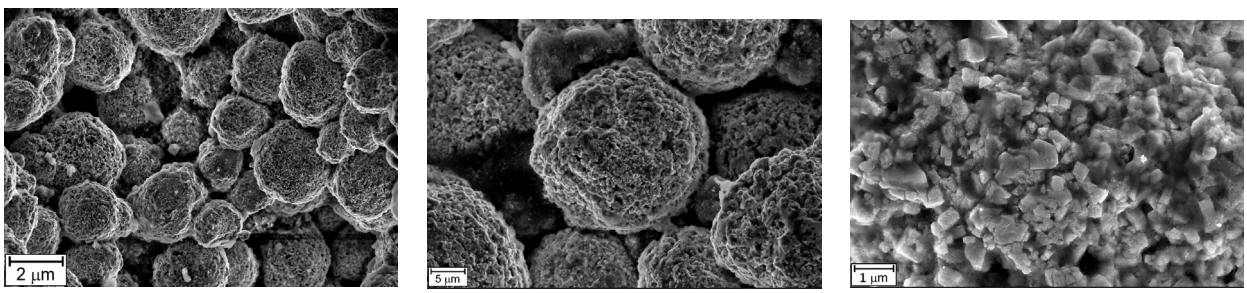

(a) (b) (c)

Fig.1. Thermal spray powder at different magnifications. (a) ×2k; (b) ×5k; (c) ×30k.

the coating. These hard WC particles reflect on the high hardness of the coating, which was measured as HV 1381. The porosity of the coating is about 0.2%. Thermal sprayed coatings by HVOF usually exhibit dense microstructure with porosity less than 1%. These good coating properties indicated that the spray parameters were suitable for spraying this powder.

3.2 XRD analysis

It was reported that the superior corrosion resistance of the WC-Co coating was due to the Co-W-C phase (e.g., Co_3W_3C and Co_6W_6C) and the formation of the Co-W-C phase was caused by the reaction of WC and Co[10]. Fig.4 shows the X-ray diffraction patterns of the WC-Co powder as well as its coating used in this study. There is Co-W-C phase found neither in the powder nor in the coating. It has been reported that the as-sprayed WC-Co coating had an amorphous phase form at a diffraction angle of approximately 43°. From Fig.4, there seems to be a shallow and broad peak between 38° and 45°. This amorphous phase is assumed to be the W_2C phase caused by the decarburization of WC during the spraying process[12,13]. It is also reported that with extra annealing at 873K, the amorphous phase is possible to crystallize to Co_6W_6C, metallic cobalt and tungsten[14]. However, the coating is not treated or used at such a high temperature. The coating in this study is assumed to have no Co-W-C phase included.

3.3 Corrosion Resistance

Fig.5 shows the coating conditions of the sample before and after testing. There were three testing cycles and each testing cycle was about two weeks. After the

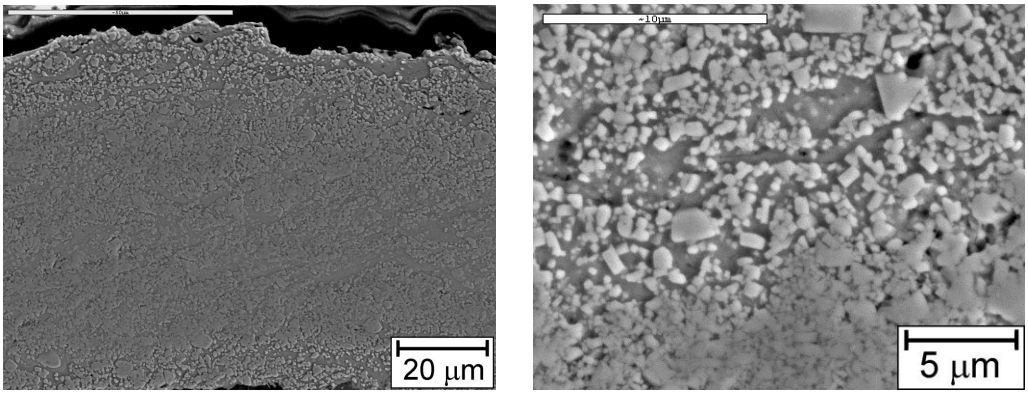

(a) (b)

Fig.3. Microstructure of the WC-Co coating. (a) Coating thickness is about 75μm; (b) WC particles are distributed in the coating.

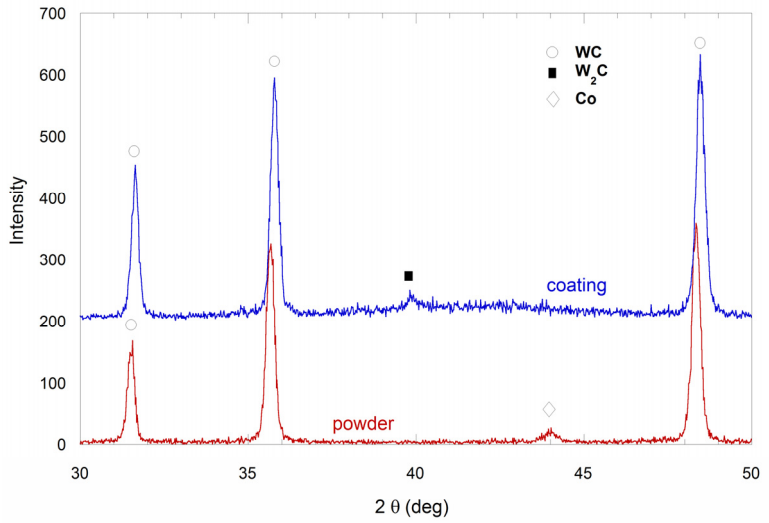

Fig.4. XRD analysis of the WC-Co powder and coating.

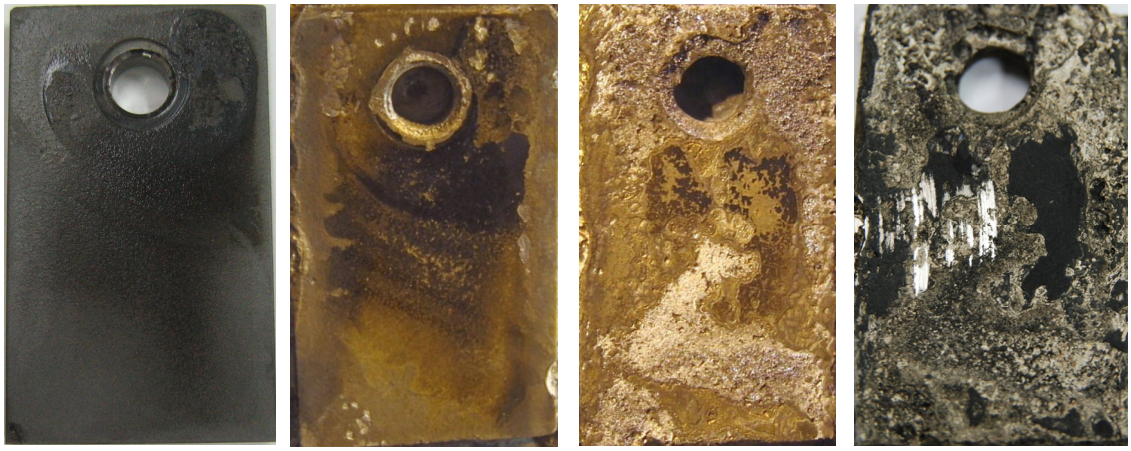

(a) (b) (c) (d)

Fig.5. Coating conditions before and after testing. (a)Before testing; (b)After the 1st cycle; (c) After the 2nd cycles; (d) After the 3rd cycles.

first testing cycle, there were minor pits around the sample peripheral. After the second testing cycle, large area spallation was found. When the third testing cycle was done, only about 18% of the coating was remained. Examining the remained coating, it was found that its thickness was almost the same with that of before testing.

It was reported that the Co phase binder would dissolve in molten zinc and deteriorate the WC-Co coating[8,10,11]. If this is the case, WC particles near the coating surface could fall out easily once the Co phase started dissolving. When the outer WC particles detached from the coating, a new layer of WC particles with Co phase binder would again be exposed to molten zinc and the deterioration process repeated. The dissolution should cause uniform thinning of the coating. However, there was some coating almost unattacked while other had gone and revealed the substrate.

3.4 Corrosion Morphologies

The tested sample was cross-sectioned and examined by SEM. Two major corrosion morphologies were found. They are dissolution of Co phase and corrosion crack.

Fig.6 shows the dissolution of Co phase near the coating surface. When the Co phase dissolved into the molten zinc, the WC particles lost the binder and were detached from the coating, resulting in the decrease of the coating thickness. This is the major mechanism reported in the literature[11]. However, if this is the major reason causing the degradation of the coating, it should be a kind of uniform corrosion. The coating should be thinning uniformly. But it was found that there was still some coating remained unattacked while others had totally gone.

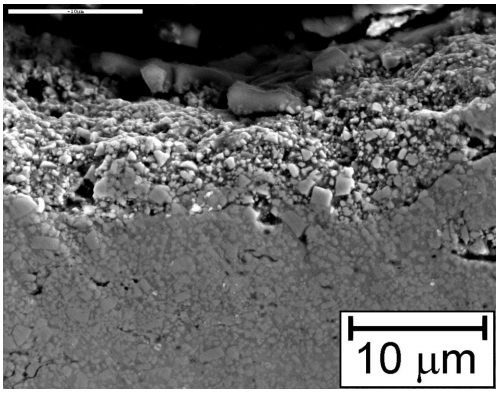

Fig.6. Dissolution of Co phase near the coating surface.

Fig.7 shows the corrosion cracks in the coating. There are both transverse and longitudinal cracks. The longitudinal crack may connect with other longitudinal ones or part of the transverse ones to cause large area decomposition. It is questioned that these cracks might be caused from the sampling preparation. However, there is dissolution of Co phase or diffusion of Zn inside the cracks which indicate that these cracks were form when immersing in the zinc pot.

The transverse crack provides a passage for the molten zinc intrusion directly to the substrate. Through the passage, the dissolution of Co phase also occurred inside the coating, as circled in Fig.8. Fig.9 shows one of the transverse cracks and its elemental mapping. From the Co map, the dissolution of Co phase was found inside the coating. From the Zn and Fe maps, zinc was found to intrude the substrate through the crack and caused the dissolution of Fe on the substrate. It is likely to weaken the adhesion strength of the coating.

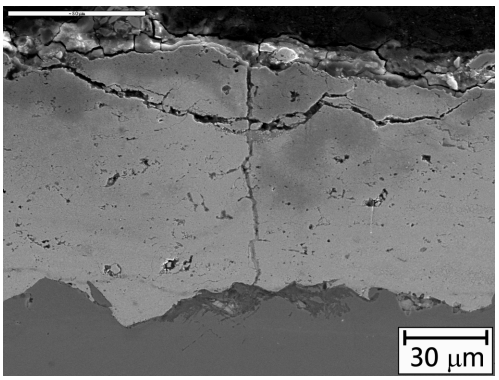

Fig.7. Corrosion cracks.

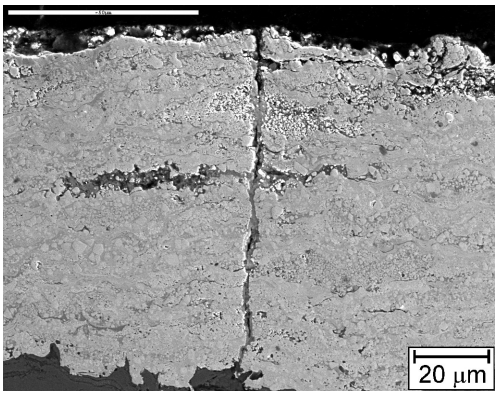

Fig.8. A transverse crack in the coating.

Except through the transverse cracks, the molten zinc was found to attack the substrate from the sample edge or the coating detached area, where the substrate had direct contact with the molten zinc. Fig.10 shows the cross section of the coating. The left side coating was corroded and detached from the substrate. There was significant dissolution of Fe found beneath the remaining coating. Here the dissolution of Fe was most likely by the molten zinc attack from the coating detached area, but not from the transverse cracks. The transverse crack, instead, would connect with the weakened interface and play a role for next large coating area destruction.

3.5 Corrosion of a Sink Roll

Fig.11 shows a used sink roll with a lot of pits on the roll surface. This roll was thermal sprayed with WC-Co coating although the actual composition of the coating was not known. It has been using in a zinc pot for a few weeks before it was pickled to remove the zinc dross. This kind of pit was also shown on the sample after the first cycle test (Fig.5(b)). Fig.12 is a higher magnification showing the corrosion condition of the coating. It can be seen that this sink roll was sculptured with narrow grooves. The coating was partially corroded. There was coating spallation on selected areas and most of them were on the convex of the grooves.

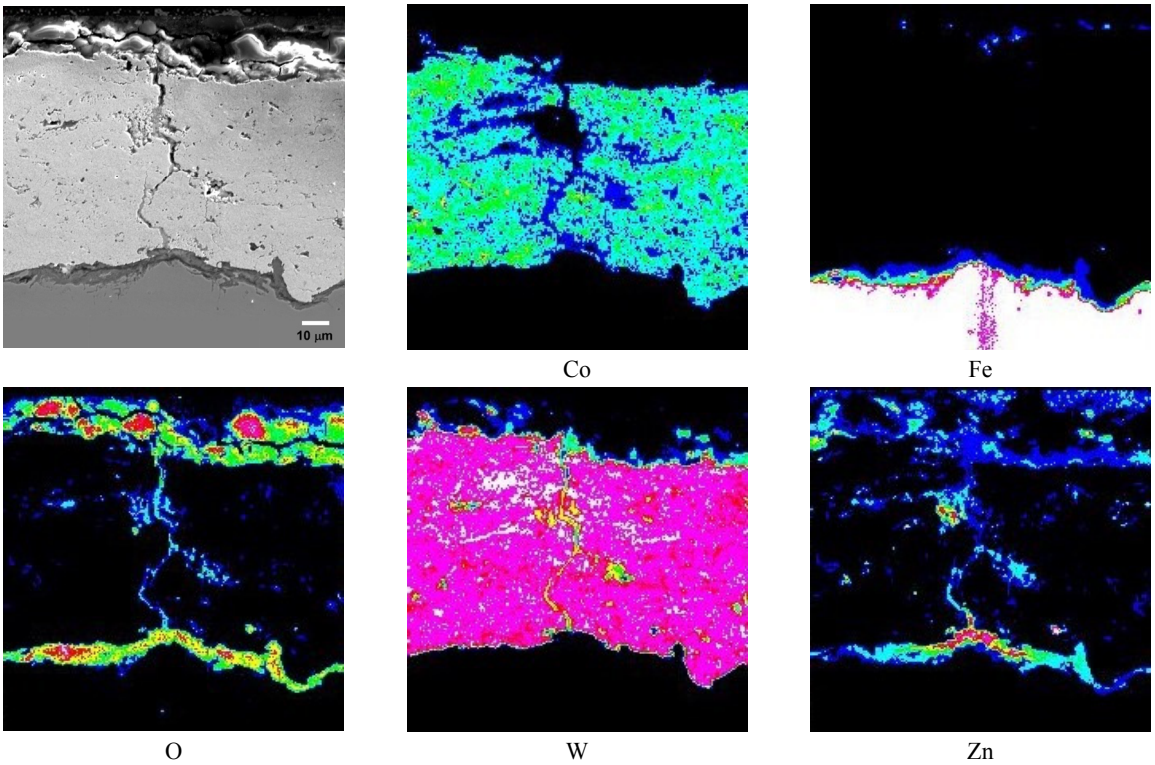

Fig.9. EPMA analysis of a corrosion crack in the coating.

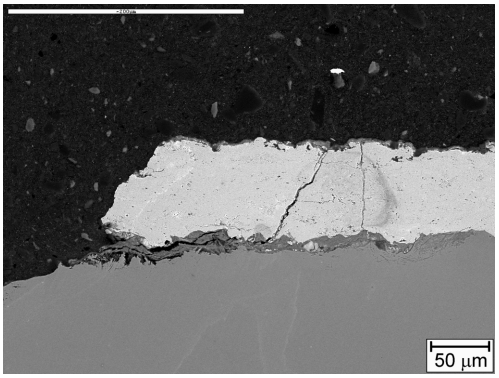

Fig.10. Cross section of the coating showing the damage of the coating.

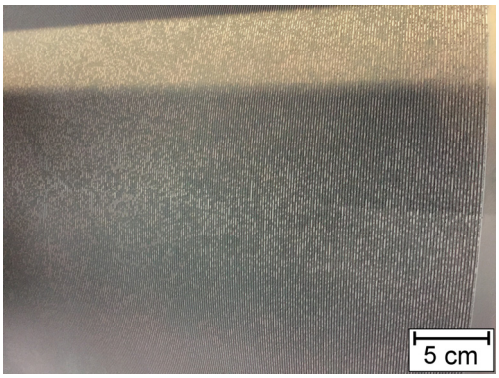

Fig.11. A corroded sink roll.

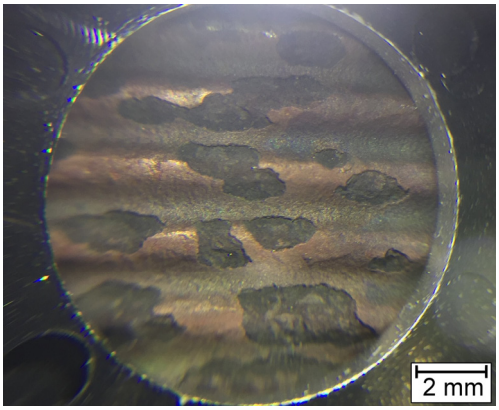

Fig.12. The coating on the grooves has selected area corroded.

Fig.13 shows the detail of the coating spallation. It seems that the whole coating was missing and revealed the substrate at the corroded area. The uncorroded area kept a certain thickness of the coating. Therefore, it is not uniformly corroded. It is rather selectively corroded by large coating area destruction.

3.6 Corrosion Mechanism

The dissolution of Co phase in WC-Co coating was found in this study; however, the degradation of the coating was not uniformly attenuated. Therefore, the dissolution of Co phase should not be the main corrosion mechanism. It was found that the large coating area detachment contributed to the destruction of the coating, both on the samples or on the sink roll. It is caused by the intrusion of molten zinc to dissolve Fe in the substrate which weakens the adhesion strength of the coating. The intrusion of zinc is from either the transverse cracks in the coating or the coating edge where the substrate has direct contact with the molten zinc. Once the substrate is attacked by the molten zinc, the coating above it is likely to combine with other transverse cracks and be detached from the substrate.

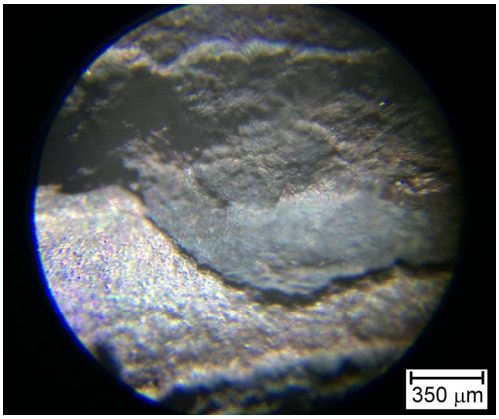

Fig.13. The missing coating reveals the substrate while the remaining coating still has a certain thickness.

3.7 Strategy and Improvement

With fully understanding of the corrosion mechanism, several attempts have been made to solve the problem. Among them, a special post-treatment after thermal spraying has shown to be highly effective. It helps to seal the cracks and micro-cracks of the thermal sprayed coating, which greatly retards the intrusion of molten zinc. After several on-site tests, the service life of the thermal spayed sink roll was proven to have been lengthened.

4. CONCLUSIONS

The thermal sprayed WC-Co coating was tested in molten zinc. The corrosion morphologies of the coating were investigated. A used sink roll was also observed and its corrosion condition was compared with that on the samples. A few conclusions are made.

1. Dissolution of Co phase and corrosion crack are two major corrosion morphologies.
2. Dissolution of Co phase may occur not only on the surface, but also inside the coating if there is a crack as a passage for molten zinc.
3. Corrosion cracks may be transverse or longitudinal. The transverse cracks may connect with other cracks to cause large coating area decomposition.

The longitudinal crack provides a passage for molten zinc to attack the substrate.

4. The key factor causing the deterioration of the WC-Co coating is rather corrosion crack but dissolution of Co phase. Both the sample and the sink roll had selective corrosion but not uniform corrosion.
5. With a special post-treatment after thermal spraying, corrosion of the coating can be greatly reduced and the life of the sink roll can be lengthened.

REFERENCES

1. A. R. Mardera: Prog. Mater. Sci., 2000, 45 (3), pp. 191-271.
2. K. Zhang, N. Y. Tang, F. E. Goodwin, and S. Sexton: J. Mater. Sci., 2007, 42 (23), pp. 9736-9745.
3. X. Liu, E. Barbero, J. Xu, M. Burris, K. Chang, and V. Sikka: Metall. Mater. Trans. A, 2005, 36A (8), pp. 2049-2058.
4. M. Bright: "Investigation Galvanneal Reactions on Pot Hardware Materials", pp. 661-668 in Proc. AISTech conference, Indianapolis, USA, May 5-7, 2007.
5. K. Zhang, and N. Tang: Mater. Sci. Technol., 2004, 20 (6), pp. 739-746.
6. M. Sawa, and J. Oohori: "Application of Thermal Spraying Technology at Steel Works", pp. 37-42 in Proc. International Thermal Spraying Conference, Kobe, Japan, May 22-26, 1995.
7. H. H. Fukubayashi: "Present Furnace and Pot Roll Coatings and Future Development", pp. 125-131, in Proc. International Thermal Spraying Conference, Osaka, Japan, May 10-12, 2004.
8. B. G. Seong, S. Y. Hwang, M. C. Kim, and K. Y. Kim: Surf. Coat. Technol., 2001, 138 (1), pp. 101-110.
9. Y. Dong, D. Yan, J. He, J. Zhang, and X. Li: Surf. Coat. Technol., 2006, 201 (6), pp. 2455-2459.
10. T. TOMITA, Y. TAKATANI, Y. KOBAYASHI, Y. HARADA, and H. NAKAHIRA: ISIJ International, 1993, 33 (9), pp. 982-988.
11. K. TANI, T. TOMITA, Y. KOBAYASHI, Y. TAKATANI, and Y. HARADA: ISIJ International, 1994, 34 (10), pp. 822-828.
12. Z.-G. Ban, and L. L. Shaw: J. Therm. Spray Technol., 2003, 12 (1), pp. 112-119.
13. G. V. Samsonov, and I. M. Vinitskii: Handbook of Refractory Compounds, IFI/Plenum Data Co., 1980.
14. C. J. Li, A. Ohmori and Y. Harada: J. Therm. Spray Technol., 1996, 5 (3), pp. 69-73. □